Title
Charmed hadron production at low transverse momentum in Au+Au collisions at RHIC

Author
Abelev, BI

Publication Date
2008-05-03

Peer reviewed

Charmed hadron production at low transverse momentum in Au+Au collisions at RHIC

B.I. Abelev,[9] M.M. Aggarwal,[30] Z. Ahammed,[45] B.D. Anderson,[20] D. Arkhipkin,[13] G.S. Averichev,[12] Y. Bai,[28] J. Balewski,[17] O. Barannikova,[9] L.S. Barnby,[2] J. Baudot,[18] S. Baumgart,[50] V.V. Belaga,[12] A. Bellingeri-Laurikainen,[40] R. Bellwied,[48] F. Benedosso,[28] R.R. Betts,[9] S. Bhardwaj,[35] A. Bhasin,[19] A.K. Bhati,[30] H. Bichsel,[47] J. Bielcik,[50] J. Bielcikova,[50] L.C. Bland,[3] S-L. Blyth,[22] M. Bombara,[2] B.E. Bonner,[36] M. Botje,[28] J. Bouchet,[40] A.V. Brandin,[26] T.P. Burton,[2] M. Bystersky,[11] X.Z. Cai,[39] H. Caines,[50] M. Calderón de la Barca Sánchez,[6] J. Callner,[9] O. Catu,[50] D. Cebra,[6] M.C. Cervantes,[41] Z. Chajecki,[29] P. Chaloupka,[11] S. Chattopadhyay,[45] H.F. Chen,[38] J.H. Chen,[39] J.Y. Chen,[49] J. Cheng,[43] M. Cherney,[10] A. Chikanian,[50] W. Christie,[3] S.U. Chung,[3] R.F. Clarke,[41] M.J.M. Codrington,[41] J.P. Coffin,[18] T.M. Cormier,[48] M.R. Cosentino,[37] J.G. Cramer,[47] H.J. Crawford,[5] D. Das,[45] S. Dash,[15] M. Daugherity,[42] M.M. de Moura,[37] T.G. Dedovich,[12] M. DePhillips,[3] A.A. Derevschikov,[32] L. Didenko,[3] T. Dietel,[14] P. Djawotho,[17] S.M. Dogra,[19] X. Dong,[22] J.L. Drachenberg,[41] J.E. Draper,[6] F. Du,[50] V.B. Dunin,[12] J.C. Dunlop,[3] M.R. Dutta Mazumdar,[45] W.R. Edwards,[22] L.G. Efimov,[12] V. Emelianov,[26] J. Engelage,[5] G. Eppley,[36] B. Erazmus,[40] M. Estienne,[18] P. Fachini,[3] R. Fatemi,[23] J. Fedorisin,[12] A. Feng,[49] P. Filip,[13] E. Finch,[50] V. Fine,[3] Y. Fisyak,[3] J. Fu,[49] C.A. Gagliardi,[41] L. Gaillard,[2] M.S. Ganti,[45] E. Garcia-Solis,[9] V. Ghazikhanian,[7] P. Ghosh,[45] Y.N. Gorbunov,[10] H. Gos,[46] O. Grebenyuk,[28] D. Grosnick,[44] B. Grube,[34] S.M. Guertin,[7] K.S.F.F. Guimaraes,[37] A. Gupta,[19] N. Gupta,[19] B. Haag,[6] T.J. Hallman,[3] A. Hamed,[41] J.W. Harris,[50] W. He,[17] M. Heinz,[50] T.W. Henry,[41] S. Heppelmann,[31] B. Hippolyte,[18] A. Hirsch,[33] E. Hjort,[22] A.M. Hoffman,[23] G.W. Hoffmann,[42] D.J. Hofman,[9] R.S. Hollis,[9] M.J. Horner,[22] H.Z. Huang,[7] E.W. Hughes,[4] T.J. Humanic,[29] G. Igo,[7] A. Iordanova,[9] P. Jacobs,[22] W.W. Jacobs,[17] P. Jakl,[11] P.G. Jones,[2] E.G. Judd,[5] S. Kabana,[40] K. Kang,[43] J. Kapitan,[11] M. Kaplan,[8] D. Keane,[20] A. Kechechyan,[12] D. Kettler,[47] V.Yu. Khodyrev,[32] J. Kiryluk,[22] A. Kisiel,[29] E.M. Kislov,[12] S.R. Klein,[22] A.G. Knospe,[50] A. Kocoloski,[23] D.D. Koetke,[44] T. Kollegger,[14] M. Kopytine,[20] L. Kotchenda,[26] V. Kouchpil,[11] K.L. Kowalik,[22] P. Kravtsov,[26] V.I. Kravtsov,[32] K. Krueger,[1] C. Kuhn,[18] A.I. Kulikov,[12] A. Kumar,[30] P. Kurnadi,[7] A.A. Kuznetsov,[12] M.A.C. Lamont,[50] J.M. Landgraf,[3] S. Lange,[14] S. LaPointe,[48] F. Laue,[3] J. Lauret,[3] A. Lebedev,[3] R. Lednicky,[13] C-H. Lee,[34] S. Lehocka,[12] M.J. LeVine,[3] C. Li,[38] Q. Li,[48] Y. Li,[43] G. Lin,[50] X. Lin,[49] S.J. Lindenbaum,[27] M.A. Lisa,[29] F. Liu,[49] H. Liu,[38] J. Liu,[36] L. Liu,[49] T. Ljubicic,[3] W.J. Llope,[36] R.S. Longacre,[3] W.A. Love,[3] Y. Lu,[49] T. Ludlam,[3] D. Lynn,[3] G.L. Ma,[39] J.G. Ma,[7] Y.G. Ma,[39] D.P. Mahapatra,[15] R. Majka,[50] L.K. Mangotra,[19] R. Manweiler,[44] S. Margetis,[20] C. Markert,[42] L. Martin,[40] H.S. Matis,[22] Yu.A. Matulenko,[32] T.S. McShane,[10] A. Meschanin,[32] J. Millane,[23] M.L. Miller,[23] N.G. Minaev,[32] S. Mioduszewski,[41] A. Mischke,[28] J. Mitchell,[36] B. Mohanty,[22] D.A. Morozov,[32] M.G. Munhoz,[37] B.K. Nandi,[16] C. Nattrass,[50] T.K. Nayak,[45] J.M. Nelson,[2] C. Nepali,[20] P.K. Netrakanti,[33] L.V. Nogach,[32] S.B. Nurushev,[32] G. Odyniec,[22] A. Ogawa,[3] V. Okorokov,[26] D. Olson,[22] M. Pachr,[11] S.K. Pal,[45] Y. Panebratsev,[12] A.I. Pavlinov,[48] T. Pawlak,[46] T. Peitzmann,[28] V. Perevoztchikov,[3] C. Perkins,[5] W. Peryt,[46] S.C. Phatak,[15] M. Planinic,[51] J. Pluta,[46] N. Poljak,[51] N. Porile,[33] A.M. Poskanzer,[22] M. Potekhin,[3] E. Potrebenikova,[12] B.V.K.S. Potukuchi,[19] D. Prindle,[47] C. Pruneau,[48] N.K. Pruthi,[30] J. Putschke,[22] I.A. Qattan,[17] R. Raniwala,[35] S. Raniwala,[35] R.L. Ray,[42] D. Relyea,[4] A. Ridiger,[26] H.G. Ritter,[22] J.B. Roberts,[36] O.V. Rogachevskiy,[12] J.L. Romero,[6] A. Rose,[22] C. Roy,[40] L. Ruan,[3] M.J. Russcher,[28] R. Sahoo,[15] I. Sakrejda,[22] T. Sakuma,[23] S. Salur,[50] J. Sandweiss,[50] M. Sarsour,[41] P.S. Sazhin,[12] J. Schambach,[42] R.P. Scharenberg,[33] N. Schmitz,[24] J. Seger,[10] I. Selyuzhenkov,[48] P. Seyboth,[24] A. Shabetai,[18] E. Shahaliev,[12] M. Shao,[38] M. Sharma,[30] W.Q. Shen,[39] S.S. Shimanskiy,[12] E.P. Sichtermann,[22] F. Simon,[23] R.N. Singaraju,[45] N. Smirnov,[50] R. Snellings,[28] P. Sorensen,[3] J. Sowinski,[17] J. Speltz,[18] H.M. Spinka,[1] B. Srivastava,[33] A. Stadnik,[12] T.D.S. Stanislaus,[44] D. Staszak,[7] R. Stock,[14] M. Strikhanov,[26] B. Stringfellow,[33] A.A.P. Suaide,[37] M.C. Suarez,[9] N.L. Subba,[20] M. Sumbera,[11] X.M. Sun,[22] Z. Sun,[21] B. Surrow,[23] T.J.M. Symons,[22] A. Szanto de Toledo,[37] J. Takahashi,[37] A.H. Tang,[3] T. Tarnowsky,[33] J.H. Thomas,[22] A.R. Timmins,[2] S. Timoshenko,[26] M. Tokarev,[12] T.A. Trainor,[47] S. Trentalange,[7] R.E. Tribble,[41] O.D. Tsai,[7] J. Ulery,[33] T. Ullrich,[3] D.G. Underwood,[1] G. Van Buren,[3] N. van der Kolk,[28] M. van Leeuwen,[22] A.M. Vander Molen,[25] R. Varma,[16] I.M. Vasilevski,[13] A.N. Vasiliev,[32] R. Vernet,[18] S.E. Vigdor,[17] Y.P. Viyogi,[15] S. Vokal,[12] S.A. Voloshin,[48] M. Wada,[10] W.T. Waggoner,[10] F. Wang,[33] G. Wang,[7] J.S. Wang,[21] X.L. Wang,[38] Y. Wang,[43] J.C. Webb,[44] G.D. Westfall,[25] C. Whitten Jr.,[7] H. Wieman,[22] S.W. Wissink,[17] R. Witt,[50] J. Wu,[38] Y. Wu,[49] N. Xu,[22] Q.H. Xu,[22] Z. Xu,[3] P. Yepes,[36] I-K. Yoo,[34] Q. Yue,[43] V.I. Yurevich,[12] M. Zawisza,[46] W. Zhan,[21] H. Zhang,[3] W.M. Zhang,[20] Y. Zhang,[38] Z.P. Zhang,[38]

Y. Zhao,[38] C. Zhong,[39] J. Zhou,[36] R. Zoulkarneev,[13] Y. Zoulkarneeva,[13] A.N. Zubarev,[12] and J.X. Zuo[39]
(STAR Collaboration)

[1] *Argonne National Laboratory, Argonne, Illinois 60439*
[2] *University of Birmingham, Birmingham, United Kingdom*
[3] *Brookhaven National Laboratory, Upton, New York 11973*
[4] *California Institute of Technology, Pasadena, California 91125*
[5] *University of California, Berkeley, California 94720*
[6] *University of California, Davis, California 95616*
[7] *University of California, Los Angeles, California 90095*
[8] *Carnegie Mellon University, Pittsburgh, Pennsylvania 15213*
[9] *University of Illinois at Chicago, Chicago, Illinois 60607*
[10] *Creighton University, Omaha, Nebraska 68178*
[11] *Nuclear Physics Institute AS CR, 250 68 Řež/Prague, Czech Republic*
[12] *Laboratory for High Energy (JINR), Dubna, Russia*
[13] *Particle Physics Laboratory (JINR), Dubna, Russia*
[14] *University of Frankfurt, Frankfurt, Germany*
[15] *Institute of Physics, Bhubaneswar 751005, India*
[16] *Indian Institute of Technology, Mumbai, India*
[17] *Indiana University, Bloomington, Indiana 47408*
[18] *Institut de Recherches Subatomiques, Strasbourg, France*
[19] *University of Jammu, Jammu 180001, India*
[20] *Kent State University, Kent, Ohio 44242*
[21] *Institute of Modern Physics, Lanzhou, China*
[22] *Lawrence Berkeley National Laboratory, Berkeley, California 94720*
[23] *Massachusetts Institute of Technology, Cambridge, MA 02139-4307*
[24] *Max-Planck-Institut für Physik, Munich, Germany*
[25] *Michigan State University, East Lansing, Michigan 48824*
[26] *Moscow Engineering Physics Institute, Moscow Russia*
[27] *City College of New York, New York City, New York 10031*
[28] *NIKHEF and Utrecht University, Amsterdam, The Netherlands*
[29] *Ohio State University, Columbus, Ohio 43210*
[30] *Panjab University, Chandigarh 160014, India*
[31] *Pennsylvania State University, University Park, Pennsylvania 16802*
[32] *Institute of High Energy Physics, Protvino, Russia*
[33] *Purdue University, West Lafayette, Indiana 47907*
[34] *Pusan National University, Pusan, Republic of Korea*
[35] *University of Rajasthan, Jaipur 302004, India*
[36] *Rice University, Houston, Texas 77251*
[37] *Universidade de Sao Paulo, Sao Paulo, Brazil*
[38] *University of Science & Technology of China, Hefei 230026, China*
[39] *Shanghai Institute of Applied Physics, Shanghai 201800, China*
[40] *SUBATECH, Nantes, France*
[41] *Texas A&M University, College Station, Texas 77843*
[42] *University of Texas, Austin, Texas 78712*
[43] *Tsinghua University, Beijing 100084, China*
[44] *Valparaiso University, Valparaiso, Indiana 46383*
[45] *Variable Energy Cyclotron Centre, Kolkata 700064, India*
[46] *Warsaw University of Technology, Warsaw, Poland*
[47] *University of Washington, Seattle, Washington 98195*
[48] *Wayne State University, Detroit, Michigan 48201*
[49] *Institute of Particle Physics, CCNU (HZNU), Wuhan 430079, China*
[50] *Yale University, New Haven, Connecticut 06520*
[51] *University of Zagreb, Zagreb, HR-10002, Croatia*

(Dated: January 12, 2018)

We report measurements of charmed hadron production from hadronic ($D \to K\pi$) and semileptonic (μ and e) decays in 200 GeV Au+Au collisions at RHIC. Analysis of the spectra indicates that charmed hadrons have a different radial flow pattern from light or multi-strange hadrons. Charm cross sections at mid-rapidity are extracted by combining the three independent measurements, covering the transverse momentum range that contributes to ∼90% of the integrated cross section. The cross sections scale with number of binary collisions of the initial nucleons, a signature of charm production exclusively at the initial impact of colliding heavy ions. The implications for charm quark interaction and thermalization in the strongly interacting matter are discussed.

PACS numbers: 25.75.Dw, 13.20.Fc, 13.25.Ft, 24.85.+p

Charm quarks are a unique tool to probe the partonic matter created in relativistic heavy-ion collisions at RHIC energies. Due to their large mass ($\simeq$1.3 GeV/c^2), charm quarks are predicted to lose less energy than light quarks by gluon radiation in the medium [1]. In contrast, recent measurements of the p_T distributions and nuclear modification factors of non-photonic electrons (NPE) from heavy quark decays at high p_T show a suppression level similar to light hadrons [2]. This observation renews the interest in charm production and the interactions of heavy charm quarks with the hot and dense matter produced in nuclear collisions at RHIC.

Measurements of charm production at low p_T, in particular radial and elliptic flow, probe the QCD medium at thermal scales and are thus sensitive to bulk medium properties like density and the drag constant or viscosity. Model treatments for low-p_T charm production, such as energy loss by collisional dissociation [3] and in-medium transport using a diffusion formalism (in analog to Brownian motion) and resonance cross sections [4], can be used to infer transport properties such as interaction cross sections and the medium density. Calculations of charm transport in strongly coupling theories using AdS/CFT correspondence [5] may allow to further determine the viscosity or drag coefficient of quark-gluon matter formed at RHIC. Ultimately, charm quark radial flow may help establish whether light quarks thermalize [6].

These considerations often assume that charm quarks are produced only in the early stages and their production rate is reliably calculable by perturbative QCD [7, 8]. Studies of the binary collision ($N_{\rm bin}$ from Glauber model) scaling of the total charm cross section from d+Au to Au+Au collisions can be used to test these assumptions and determine if charm is indeed a good probe with well-defined initial states. The total charm production cross section is also an important input in models of J/ψ production via charm quark coalescence in a Quark Gluon Plasma [9].

In this paper, we present the study of charm via measurements of very low p_T muons [10]($0.17 \leq p_T \leq 0.25$ GeV/c), $D^0 \rightarrow K\pi$ at low p_T ($p_T \leq 2$ GeV/c), and NPE ($0.9 \leq p_T \leq 5$ GeV/c). The combination of these three techniques provides the most complete kinematic coverage ($\sim$90%) to date for charm production measurements at RHIC. They also allow the study of the charmed hadron spectral shape in order to explore the possibility of charm radial flow in Au+Au collisions.

The data used for these analyses were taken with the STAR experiment [11] during the $\sqrt{s_{\rm NN}}$ = 200 GeV Au+Au run in 2004 at RHIC. The most central 0$-$80% of the total hadronic cross section as selected using the uncorrected charged particle multiplicity at mid-rapidity ($|\eta| < 0.5$), is used for the minimum bias (minbias) measurement. A total of 13.3 million minbias triggered events were used for the D^0 reconstruction. A separate sample of central events was taken using an online selection of the 0$-$12% most central events based on the energy deposited in the two Zero-Degree Calorimeters [12]. For muons and NPE analysis, 15 million central (0$-$12%) and 7.8 million minbias triggered events are used. All measurements are presented as an average of particle and anti-particle yields at mid-rapidity ($|y| < 1$ for D^0 and $-1 < y < 0$ for $\mu(e)$ limited by the TOF detector acceptance.).

D^0 mesons were reconstructed through their decay $D^0(\bar{D^0}) \rightarrow K^{\mp}\pi^{\pm}$ with a branching ratio of 3.83%. The analysis is identical to that used for d+Au collisions [13]. An example invariant mass distribution after subtraction of the combinatorial background from mixed events is shown in Fig. 1(a) (full circles). The D^0 yield is extracted by fitting a Gaussian peak plus a linear or second-order polynomial to describe the residual background to the measured distribution (red curve in Fig. 1 (a)). The total systematic uncertainty on D^0 yield bin-by-bin is $\sim$40$-$50%, evaluated by varying the particle identification conditions and yield extraction procedures.

Muons were identified by combining the Time Of Flight (TOF) and ionization energy loss (dE/dx) measured in the Time Projection Chamber (TPC) [10, 12, 13]. Fig. 1(b) shows the m^2 distribution from TOF for tracks with $0.17 \leq p_T \leq 0.21$ GeV/c. Muons are selected in the range $0.008 \leq m^2 \leq 0.014$ GeV^2/c^4. The distribution of the distance of closest approach (DCA) of the tracks to the primary vertex is used to further separate μ from charm decay and from pion and kaon decays. Fig. 1(c) shows the DCA distribution of μ after a statistical subtraction of the DCA distribution from misidentified pions [14]. The remaining dominant background μ from π/K weak decays have different DCA distributions from the prompt muons, shown in Fig. 1(c). The prompt μ raw yield was obtained from a fit to the μ DCA distributions with the background DCA distribution and the primary particle DCA distribution [10]. Other sources of background ($\rho \rightarrow \mu^+\mu^-$, $\eta \rightarrow \gamma\mu^+\mu^-$, $K^0_S \rightarrow \pi\mu\nu$, etc.) are found to be negligible from simulations using yields from measured spectra at RHIC. The systematic uncertainty is dominated by the uncertainty on the pion contamination and was estimated using different dE/dx cuts for the pions.

Electrons are identified up to $p_T = 5$ GeV/c by dE/dx from TPC after applying a TOF selection $|1/\beta - 1| \leq 0.03$ [12, 13]. The 5$-$15% bin-by-bin systematic uncertainties in inclusive electron yields are dominated by the uncertainties in the raw yield extraction using different fit functions. The dominant sources of photonic electron background are photon conversions and $\pi^0(\eta)$ Dalitz decays. e^+e^- pairs from these background sources were

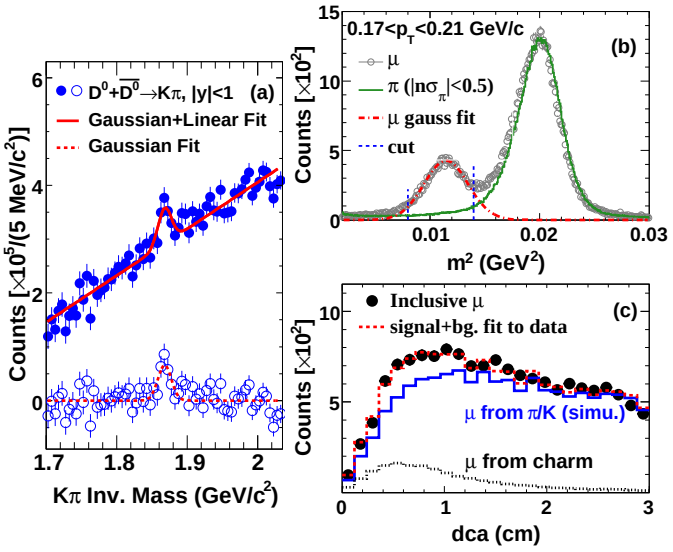

FIG. 1: (a) Kaon-pion pair invariant mass distribution for minbias Au+Au collisions, after subtraction of mixed event background (solid circles) and additional subtraction of a linear residual background (open circles). A 4σ signal is observed. (b) Mass squared distribution $m^2 = (p/\beta/\gamma)^2$ from TOF. (c) μ DCA distributions (open circles). Histograms indicate the background from π/K decays (solid curve), the contribution from prompt muons (dotted curve) and the sum (dashed curve).

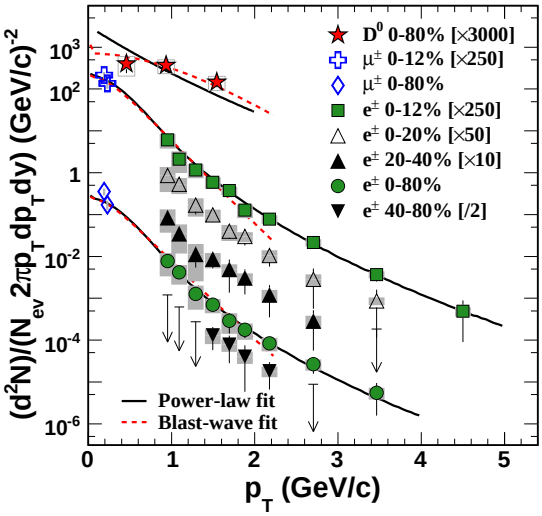

FIG. 2: p_T distributions of invariant yields for D^0, charm-decayed prompt μ and NPE in different centralities. Solid curves are power-law combined fit for D^0 and leptons. Dashed curves are blast-wave fit. The gray bands are bin-to-bin systematic uncertainties.

subtracted using an invariant mass technique [10, 13, 15]. The photonic background reconstruction efficiency was calculated in a Monte Carlo simulation of π^0 and direct photons according to the measured π^+ [16] and π^0 [17] spectra, and varies from 25% at low p_T to 60% at highest p_T in the range studied. The systematic uncertainties (7−16%) for photonic electrons are mainly from the combinatorial background uncertainties and the background reconstruction efficiency. The remaining background from photonic decays of η, ω, ρ, ϕ and K was determined to be $\lesssim$5% from simulations and is subtracted in the final result. The ratio of inclusive electrons to photonic background increases from $\sim$ 1 to 1.45 within the p_T range studied.

Fig. 2 shows the p_T spectra for D^0, μ and NPE for Au+Au minbias events. Additional centralities are shown for the semi-leptonic decay measurements. We start with a p_T spectrum function for D^0 (power-law or blast-wave functions) and obtain spectrum function from semileptonic decay for NPE and μ from that. Additional p_T-dependent factor (upper and lower bounds from FONLL [8]) is applied to the lepton function to take into account the contribution from bottom decays. These functions are used in a combined fit [18] to obtain the mid-rapidity charm yield and $\langle p_T \rangle$. The χ^2 from the fit was with systematic errors included. The correlations between systematic errors on different data points were also taken into account in the combined fit [19]. The D^0 $\langle p_T \rangle$ as calculated from power law fits are $0.92\pm0.06(stat.)\pm0.12(sys.)$ GeV/c for minbias and $0.95\pm0.04\pm0.16$ GeV/c for 0−12% central Au+Au collisions.

The nuclear modification factors ($R_{AuAu/dAu}$) [20] for μ and NPE are shown in Fig. 3. The $R_{AuAu/dAu}$ are the ratios of the p_T spectra in Au+Au and in d+Au collisions appropriately scaled with the number of binary collisions. No muon measurements were carried out for the d+Au system. The d+Au reference is the decay lepton curve from the power-law combined fit ($\langle p_T \rangle = 1.18\pm0.02\pm0.10$ GeV/$c, n = 11.5\pm0.5\pm1.5$) with D^0 and NPE from previously published data [2, 13]. The nuclear modification factor at low p_T is consistent with 1 to within the 25% relative uncertainty of the muon measurement, and then reduces at higher p_T, reaching a value similar to light hadrons at high $p_T \gtrsim 4$ GeV/c [16]. Our result is consistent with other measurements of NPE at high p_T [2]. Model calculations incorporating in-medium charm resonances/diffusion or collisional dissociation in a strongly interacting medium [3, 4, 6], which can reasonably be applied to describe the NPE spectra down to low p_T, are shown in Fig. 3.

To study whether charmed hadrons have similar radial flow to light hadrons, we have included curves for the expected nuclear modification factor from a blast-wave model, using the freeze-out parameters for light hadrons [21] (BW3 in Fig. 3) and multi-strange hadrons [22] (BW2). The data and best blast-wave fit (BW1) show large deviations from both these curves for $p_T > 1$ GeV/c, which suggests that the charmed hadron freeze-out and flow are different from light hadrons. We scanned the parameters to a 2-dimensional T_{fo}, $\langle \beta_t \rangle$ space, the results show little sensitivity to freeze-out temperature, but disfavor large radial flow. These find-

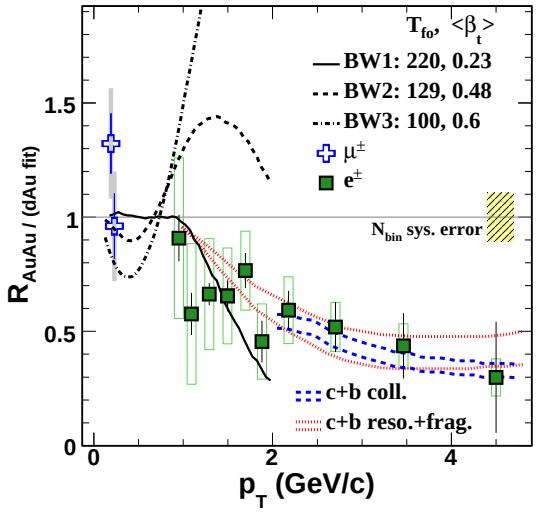

FIG. 3: Nuclear modification factor ($R_{AuAu/dAu}$) for 0−12% Au+Au collisions. Bin-to-bin systematic uncertainties are represented by the gray bands for muons and the open boxes for electrons. The shaded band at unity shows the common N_{bin} normalization uncertainties. Model calculations are presented: coalescence and fragmentation [4] (double-dotted curves), and collisional dissociation of heavy meson [3] (double-dashed curves). The curves at $p_T \leq 2$ GeV/c indicate blast-wave model with different freeze-out parameters (T_{fo} in MeV, $\langle\beta_t\rangle$) as indicated in the legend.

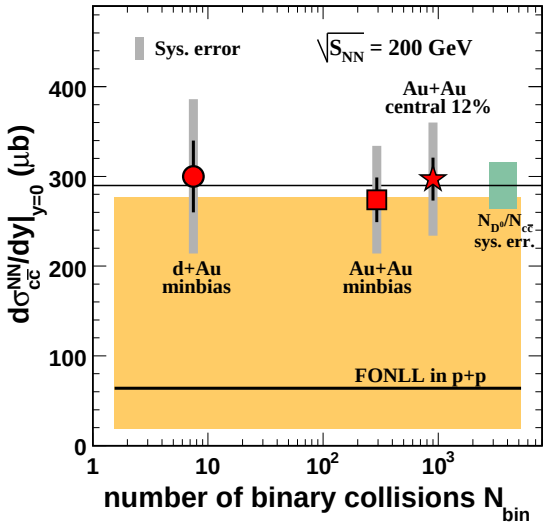

FIG. 4: Mid-rapidity charm cross section per nucleon-nucleon collision as a function of N_{bin} in d+Au, minbias and 0−12% central Au+Au collisions. The solid line indicates the average. FONLL prediction is shown as a band around the central value (thick line) [25].

ings, together with the observation of large charm elliptic flow [23], are consistent with the recent prediction from hydrodynamics [24]: elliptic flow is built up at partonic stage, and radial flow dominantly comes from hadronic scattering at later stage where charm may have already decoupled from the system.

A combined fit to the NPE and μ spectra was used to obtain the mid-rapidity charm cross section per nucleon-nucleon collision ($d\sigma_{c\bar{c}}^{NN}/dy$), shown in Fig. 4. Yields are an average from the blast-wave and the power-law functions, which are consistent within ±10%. For minbias Au+Au collisions, the D^0 data were included in the fit, assuming $N_{D^0}/N_{c\bar{c}} = 0.54\pm0.05$ [19] as is seen in p+p collisions. Fig. 4 shows $d\sigma_{c\bar{c}}^{NN}/dy$ as a function of $N_{\rm bin}$ for minbias d+Au, minbias and central Au+Au collisions. The charm production cross section at mid-rapidity scales with number of binary interactions from d+Au [13] to central Au+Au collisions. The quality of this scaling can be quantified by the slope of $d\sigma_{cc}/dy$ vs $N_{\rm bin}$ ($d\overline{\sigma_{cc}^{NN}}/dy$), which is 290 μb with ±15% uncorrelated uncertainty. This indicates that charm quarks are produced in the early stage of relativistic heavy-ion collisions. The total cross section $\sigma_{c\bar{c}}^{NN}$ (extrapolated to the full rapidity using the rapidity distribution from PYTHIA by a factor of 4.7±0.7 [13]) is 1.40±0.11±0.39 mb for central and 1.29±0.12±0.36 mb for minbias Au+Au collisions. The central values of the cross sections reported by PHENIX [23] are a factor of about two smaller than ours at all measured p_T. The difference is approximately 1.5 times the combined uncertainties. The FONLL calculation [25] is the band in Fig. 4. The ratio of the minbias data over theory calculation is $4.3\pm0.5(stat.)\pm1.2(syst.)^{+9.4}_{-3.3}(theory)$. The upper theory value reproduces our result.

In summary, we report measurements of charmed hadron production at mid-rapidity from analysis of $D \to K\pi$, $\mu(e)$ from semileptonic charm decays in minbias and central Au+Au collisions at RHIC. The blast-wave fits and the direct comparisons of the spectra suggest that charmed hadrons interact with and decouple from the system differently from the light hadrons. The $d\sigma_{c\bar{c}}^{NN}/dy$ at mid-rapidity are extracted from a combination of the three measurements covering the transverse momentum range which contributes to ∼90% of the integrated cross section. The total cross sections are found to scale with the number of binary collisions. This confirms the expected scaling of hard production processes with binary interactions among incoming nucleons so that charm quarks can be used as a calibrated probe of the early-stage dynamics of the system.

We thank the RHIC Operations Group and RCF at BNL, and the NERSC Center at LBNL for their support. This work was supported in part by the Offices of NP and HEP within the U.S. DOE Office of Science; the U.S. NSF; the BMBF of Germany; CNRS/IN2P3, RA, RPL, and EMN of France; EPSRC of the United Kingdom; FAPESP of Brazil; the Russian Ministry of Sci. and Tech.; the Ministry of Education and the NNSFC of China; IRP and GA of the Czech Republic, FOM of the Netherlands, DAE, DST, and CSIR of the Government of India; Swiss NSF; the Polish State Committee for Scien-

tific Research; Slovak Research and Development Agency, and the Korea Sci. & Eng. Foundation.

[1] Yu. L. Dokshitzer and D.E. Kharzeev, *Phys. Lett.* B **519**, 199 (2001); M. Djordjevic, M. Gyulassy and S. Wicks, *Phys. Rev. Lett.* **94**, 112301 (2005); N. Armesto, A. Dainese, C.A. Salgado and U.A. Wiedemann, *Phys. Rev.* D **71**, 054027 (2005).

[2] B. I. Abelev *et al.*, *Phys. Rev. Lett.* **98**, 192301 (2007); S. S. Adler *et al.*, *Phys. Rev. Lett.* **96**, 032301 (2006). A detailed comparison of the two sets of data points has been presented in this STAR publication.

[3] A. Adil and I. Vitev, *Phys. Lett.* B **649**, 139 (2007).

[4] R. Rapp and H. van Hees, *J. Phys.* G **32**, S351 (2006).

[5] P.K. Kovtun, D.T. Son, and A.O. Starinets, *Phys. Rev. Lett.* **94**, 111601 (2005); H. Liu, K. Rajagopal, and U.A. Wiedemann, *Phys. Rev. Lett.* **97**, 182301 (2006); C.P. Herzog *et al.*, *J. High Energy Phys.* **07**, 013 (2006); S.S. Gubser, *Phys. Rev.* D **74**, 126005 (2006); J.J. Friess, S.S. Gubser and G. Michalogiorgakis, *J. High Energy Phys.* **09**, 072 (2006).

[6] G.D. Moore and D. Teaney, *Phys. Rev.* C **71**, 064904 (2005); H. van Hees, V. Greco and R. Rapp, *Phys. Rev.* C **73**, 034913 (2006); X. Zhu *et al.*, *Phys. Lett.* B **647**, 366 (2007); N. Xu and Z. Xu, *Nucl. Phys.* A **715**, 587c (2003); Z.W. Lin and D. Molnar, *Phys. Rev.* C **68**, 044901 (2003); V. Greco, C.M. Ko and R. Rapp, *Phys. Lett.* B **595**, 202 (2004); S. Batsouli *et al.*, *Phys. Lett.* B **557**, 26 (2003).

[7] Z. Lin and M. Gyulassy, *Phys. Rev.* C **51**, 2177 (1995).

[8] M. Cacciari, P. Nason and R. Vogt, *Phys. Rev. Lett.* **95**, 122001 (2005); FONLL stands for Fixed Order plus Next-to-Leading Logarithms.

[9] P. Braun-Munzinger and J. Stachel, *Phys. Lett.* B **490**, 196 (2000); A. Andronic *et al.*, *Phys. Lett.* B **571**, 36 (2003); L. Grandchamp and R. Rapp, *Phys. Lett.* B **523**, 60 (2001); M. I. Gorenstein *et al.*, *Phys. Lett.* B **524**, 265 (2002); R.L. Thews, M. Schroedter and J. Rafelski, *Phys. Rev.* C **63**, 054905 (2001); M.I. Gorenstein *et al.*, *J. Phys.* G **28**, 2151 (2002).

[10] H.D. Liu *et al.*, *Phys. Lett.* B **639**, 441 (2006); Y. Zhang, *J. Phys.* G **32**, S529 (2006); Y. Zhang, Ph.D. Thesis, USTC/China, 2007; C. Zhong, *J. Phys.* G **34**, S741 (2007).

[11] J. Adams *et al.*, *Nucl. Phys.* A **757**, 102 (2005).

[12] K.H. Ackermann *et al.*, *Nucl. Instr. Meth.* A **499**, 624 (2003); M. Shao *et al.*, *Nucl. Instr. Meth.* A **558**, 419 (2006); M. Anderson *et al.*, *Nucl. Instr. Meth.* A **499**, 659 (2003); H. Bichsel, *Nucl. Instr. Meth.* A **562**, 154 (2006); J. Adams *et al.*, *Phys. Lett.* B **616**, 8 (2005).

[13] J. Adams *et al.*, *Phys. Rev. Lett.* **94**, 062301 (2005); X. Dong, Ph.D. thesis, e-print Arxiv: nucl-ex/0509011.

[14] A stringent dE/dx cut ($|n\sigma_\pi| < 0.5$ [10]) provides a pure pion sample. We then applied the muon m^2 window and properly normalize this background m^2 distribution to the inclusive sample at the pion mass peak. This provides the residual pion contamination which was subtracted from the μ DCA distribution.

[15] J. Adams *et al.*, *Phys. Rev.* C **70**, 044902 (2004); I. Johnson, Ph.D. thesis, U.C. Davis, 2002.

[16] J. Adams *et al.*, *Phys. Rev. Lett.* **97**, 152301 (2006).

[17] S. S. Adler *et al.*, *Phys. Rev. Lett.* **91**, 072301 (2003).

[18] The averaged $c \to l$ B.R.=9.6% was used to normalize the spectra for the fit. The differences from $c \to e$ (10.3%) and $c \to \mu$ (8.2%) were taken into account in the final systematic errors.

[19] W.-M. Yao *et al.*, *J. Phys.* G **33**, 1 (2006). When there are a number of data points of the form $A_i \pm \sigma_i \pm \Delta$ where the common systematic error is Δ, and the σ_i include the statistical error and uncorrelated (bin-to-bin) systematical error, the modified "uncorrelated" systematic error is $\Delta_i = \sigma_i \Delta [\Sigma (1/\sigma_j^2)]^{1/2}$.

[20] C. Adler *et al.*, *Phys. Rev. Lett.* **89**, 202301 (2002).

[21] J. Adams *et al.*, *Phys. Rev. Lett.* **92**, 112301 (2004).

[22] J. Adams *et al.*, *Phys. Rev. Lett.* **92**, 182301 (2004).

[23] A. Adare *et al.*, *Phys. Rev. Lett.* **97**, 252002 (2006); A. Adare *et al.*, *Phys. Rev. Lett.* **98**, 172301 (2007).

[24] T. Hirano *et al.*, e-Print: arXiv:0710.5795 [nucl-th]

[25] R. Vogt, *Int. J. Mod. Phys.* E **12**, 211 (2003); R. Vogt, e-print Arxiv: hep-ph/0709.2531.